



## ORIGINAL ARTICLE

# The effect of low-intensity cold atmospheric plasma jet on photoaging-induced hyperpigmentation in mouse model

Ga Ram Ahn MD, PhD<sup>1,2</sup>  | Hyung Joon Park MS<sup>3</sup> | Young Gue Koh MD<sup>2</sup>  |  
Ka Ram Kim MD<sup>2</sup> | Yu Jin Kim MS<sup>1</sup> | Jung Ok Lee PhD<sup>1</sup> | Joon Seok MD, PhD<sup>2</sup> |  
Kwang Ho Yoo MD, PhD<sup>4</sup> | Kyu Back Lee MD, PhD<sup>3,5</sup> | Beom Joon Kim MD, PhD<sup>1,2</sup>

<sup>1</sup>Department of Medicine, Graduate School, Chung-Ang University, Seoul, Korea

<sup>2</sup>Department of Dermatology, Chung-Ang University Hospital, Seoul, Korea

<sup>3</sup>Department of Interdisciplinary Bio/Micro System Technology, College of Engineering, Korea University, Seoul, Korea

<sup>4</sup>Department of Dermatology, Chung-Ang University Gwangmyeong Hospital, Gwangmyeong-Si, Gyeonggi-do, Korea

<sup>5</sup>School of Biomedical Engineering, Korea University, Seoul, Korea

## Correspondence

Beom Joon Kim, Department of Dermatology, 06973, Chung-Ang University Hospital, 102, Heukseok-ro, Dongjak-gu, Seoul, Korea.  
Email: [beomjoon74@gmail.com](mailto:beomjoon74@gmail.com)

## Funding information

Ministry of Science and ICT, South Korea

[Correction added on 30th June 2023, after first online publication: Affiliations 3 and 4 have been updated in this version.]

## Abstract

**Background:** Cold atmospheric plasma (CAP) produces reactive oxygen/nitrogen species (RONS) in the target and can induce cytoprotective effects by activating hormesis-related pathways when its intensity is in the low range.

**Objectives:** The aim of this study is to evaluate the effect of low-intensified CAP (LICAP) on skin with photoaging-induced hyperpigmentation in an animal model.

**Methods:** Changes in cell viability and RONS production following LICAP treatment were measured. For the in vivo study, 30 hairless mice underwent antecedent photoaging induction followed by the allocated therapy (i.e., LICAP, topical ascorbic acid (AA), or both). During the first 4 weeks of the treatment period (8 weeks), ultraviolet (UV)-B irradiation was concurrently administered. Visual inspection and measurement of the melanin index (MI) were performed to assess the change in skin pigmentation at Weeks 0, 2, 4, 6, and 8.

**Results:** RONS production increased linearly until the saturation point. Cell viability was not significantly affected by LICAP treatment. At Week 8, MI was significantly decreased in every treatment group compared with the values at Week 0 and Week 4. The treatment effect of the concurrent therapy group was superior to that of the LICAP and AA groups.

**Conclusion:** LICAP appears to be a novel modality for photoprotection and pigment reduction in photodamaged skin. LICAP treatment and topical AA application seem to exert a synergistic effect.

## KEYWORDS

cold atmospheric plasma, melanin index, photoaging, pigmentation, redox hormesis

## 1 | INTRODUCTION

After repeated or long-term exposure to ultraviolet (UV) rays, the skin undergoes photoaging. As a result, the skin becomes darker as

basal melanocytes synthesize melanosomes and transfer them to adjacent keratinocytes.<sup>1</sup> Melanosomes are important for protecting cells from UV rays to preserve skin homeostasis. However, there are always high cosmetic demands for the skin-lightening modalities.

Ga Ram Ahn, Hyung Joon Park, and Yu Jin Kim contributed equally as the first authors.

This is an open access article under the terms of the [Creative Commons Attribution](https://creativecommons.org/licenses/by/4.0/) License, which permits use, distribution and reproduction in any medium, provided the original work is properly cited.

© 2023 The Authors. *Journal of Cosmetic Dermatology* published by Wiley Periodicals LLC.

Cold atmospheric plasma (CAP) devices generate physical plasma at tissue-compatible temperatures under atmospheric conditions.<sup>2</sup> Physical plasma increases intracellular reactive species such as charged particles and reactive oxygen/nitrogen species (RONS). Based on this mechanism, cold atmospheric plasma devices have been widely used for dermatologic indications such as infection, chronic ulcer, skin barrier dysfunction, acne, scar, precancerous lesion, cancer, and skin resurfacing.<sup>3-7</sup>

Meanwhile, a growing body of evidence indicates that low-dose CAP stabilizes the cellular redox status by activating redox-sensitive transcription factors such as nuclear factor erythroid-2-related factor 2 (Nrf2), which upregulates endogenous antioxidants.<sup>8-11</sup> Moreover, such events can trigger selective autophagy,<sup>12-14</sup> which is a key process to clear the accumulated melanosomes in keratinocytes.<sup>15,16</sup>

Therefore, the present in vivo study investigated the accelerating effect of low-intensity cold atmospheric plasma jet (LICAP) on recovery from photoaging-induced hyperpigmentation and its synergistic effect with the topical antioxidant agent, L-ascorbic acid (AA), in a hairless mouse model.

## 2 | MATERIALS AND METHODS

### 2.1 | Ethics approval

The present study was performed in accordance with the guidelines of laboratory animal care of the National Institutes of Health, and the experimental protocols approved by the Chung-Ang University Institutional Animal Care and Use Committee (IACUC, No. 201900124).

### 2.2 | Quantification of reactive species production

Plasma was induced in 3 mL of phosphate-buffered saline (PBS Thermo Fisher Scientific Co.) in a 12-well plate at an 8 mm height for 5, 10, 15, 30, 60, and 120 s in order to quantify the aqueous reactive species produced in the target area. Because of its physiologic osmolality (155 mM NaCl, 2.97 mM Na<sub>2</sub>HPO<sub>4</sub>·7H<sub>2</sub>O, and 1.06 mM KH<sub>2</sub>PO<sub>4</sub>) and acidity, the PBS was chosen as the target solution for the measurement (pH 7.4). Helium gas was used as the vehicle for plasma generation. The amount of aqueous reactive species produced in the target solution was measured using the RONS assay kit (OxiSelect™, Cell Biolabs Inc.) following the manufacturer's instructions and previously published literature.<sup>17,18</sup> A 2', 7'-dichloro-dihydro-fluorescein (DCF) standard curve was used to quantify reactive species production. Briefly, 50 µL of catalyst was added to the sample along with 100 µL of DCF solution and incubated for no more than 20 min. Then, the fluorescence emitted from the redox reaction in the solution was measured using a plate reader (Gemini EM; Molecular Devices) at 480/530-nm excitation.

### 2.3 | Cell viability test

Cell viability was quantified using a colorimetric WST-1 assay. HaCaT cells (1.5 × 10<sup>5</sup>/mL; ATGC Co.) were seeded in 96-well plates and incubated at 37°C in a humidified chamber containing 5% CO<sub>2</sub>. After 24 h, 10 µL of the WST reagent was added, and spectrophotometric absorbance was measured at 450 nm.

### 2.4 | Animal model

Hairless mice were purchased from Saeron Bio Inc. in Seongnam, Korea. Six 6-week-old male HRM2-strain mice in good health were included in the study. Prior to the experiments, they were housed for 7 days under constant conditions of 55 ± 10% relative humidity, 23 °C, and a 12 h dark/12 hours light cycle.

### 2.5 | Study design

In total, 30 mice were randomized into five groups: normal control, untreated control, LICAP, ascorbic acid (AA), and LICAP + AA (Figure 1). The normal control group (group A, *n* = 6) did not undergo photoaging induction or treatment intervention. The other groups underwent photoaging induction on their dorsal skin for 12 weeks (*n* = 6, respectively) using 312-nm UV-B light from an automatic UV irradiation system (Bio-Spectra; Vilber Corp.). In this period, UV-B irradiation was performed three times a week with a gradually increasing dose from 30 to 70 mJ/cm<sup>2</sup>.

The induction period was followed by 8 weeks of the treatment period. During these 8 weeks, each treatment group (LICAP, AA, and LICAP + AA group) was subjected to the allocated treatment, three times per week. Notably, 70 mJ/cm<sup>2</sup> of UV-B was irradiated in tandem with the treatment during the first 4 weeks to observe the photoprotective effect (UV-B co-stimulation period, Weeks 0–4). After that, UV-B irradiation was discontinued to observe the recovery acceleration effect of each treatment (UV-B off period, Weeks 4–8).

### 2.6 | Treatment device

A helium plasma jet device developed by AGNES Medical Co., Ltd. was used in the study (Figure 2A,B). N50 (99.999%) helium gas was used (0.12 L/min) as the carrier. Physical plasma was generated using a 12 kHz radiofrequency with 1000 W power (peak voltage 6 kV). The generated plasma effluent was delivered to the dorsal skin of the subject for 1 min. In the concurrent therapy group (LICAP + AA), LICAP treatment was performed on dry skin before topical AA was applied.

### 2.7 | Topical ascorbic acid solution

Ascorbic acid, one of the most common active ingredients in transdermal drug delivery treatment in the dermatology field,<sup>19-23</sup> in the

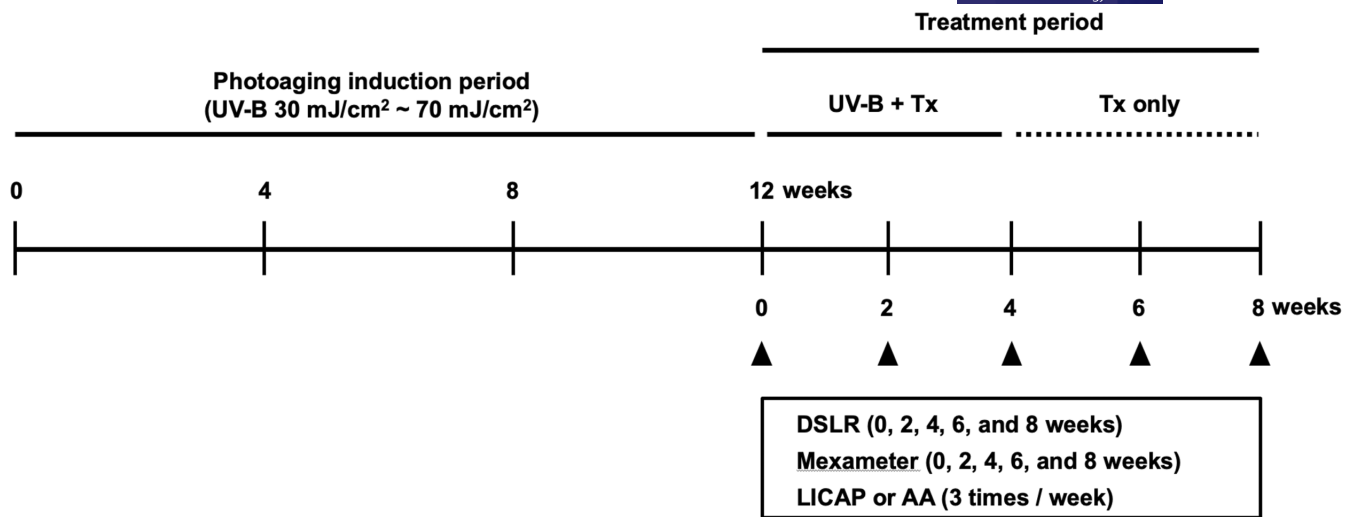


FIGURE 1 Study design for photoaging induction, treatment, and assessment.

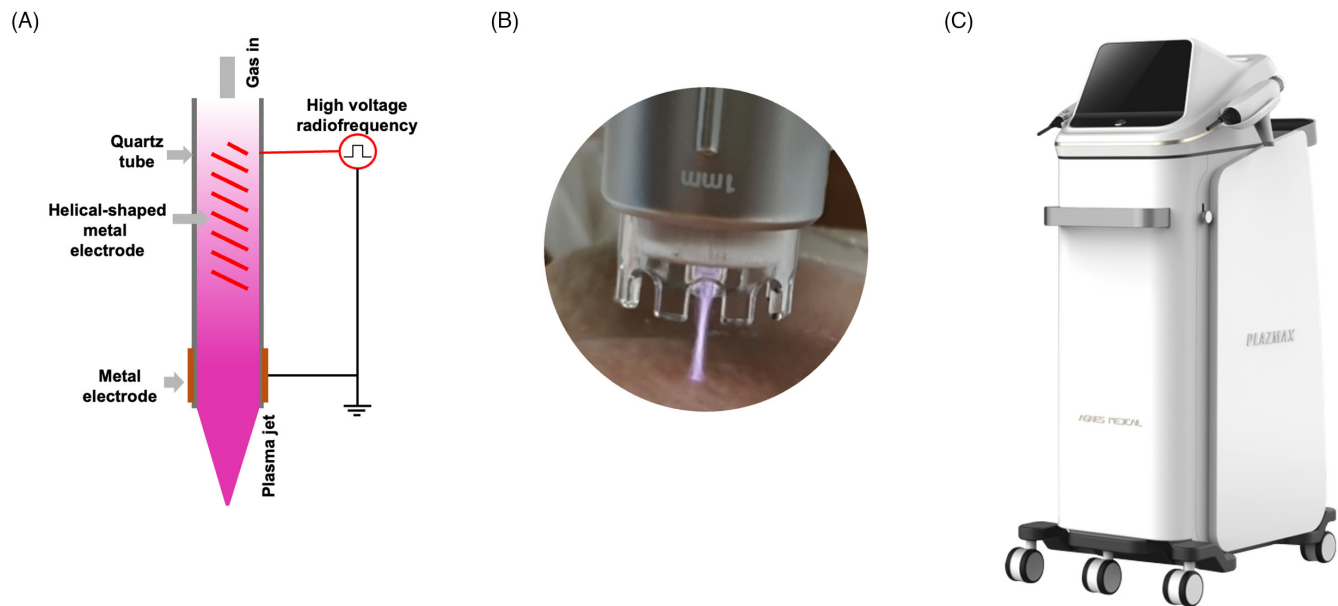


FIGURE 2 Treatment device used in the present study. (A) Scheme describing the plasma generating device with a helical shaped electrode. (B) Magnified image of plasma effluent from the device. (C) The exterior of the treatment device.

form of a solution, prepared by diluting 600mg of sodium and magnesium ascorbyl phosphate powder (Vita-C Powder™; Dermacos Korea, Co.) in 20.0mL of deionized water. For topical application, 800μL of the solution was applied to the dorsal skin of the subjects for 10min, as per the method described by the manufacturer.

## 2.8 | Assessment

The data at the baseline were assessed at 0, 2, 4, 6, and 8 weeks after the end of the induction period. The skin surface was photographed with a digital camera (EOS 300D; Canon) and was examined by a dermatologist.

The melanin index (MI) was assessed to objectively measure skin darkness using a 660-nm and 880-nm narrowband reflectance

spectrophotometer (Mexameter® MX18; Courage and Khazaka Electronic Corp.).

To present the degree of pigment reduction more clearly, the decreased percentage of melanin index from the baseline week  $i$  to a specific moment week  $j$  (DPMI <sub>$ij$</sub> ) was defined as follows:

$$\text{DPMI}_{ij} (\%) = - \frac{\text{MI at week } j - \text{MI at week } i}{\text{MI at week } i} = - \frac{\text{MI}_i - \text{MI}_j}{\text{MI}_i} \times 100$$

Two different baseline moments were set: (1) Week 0, immediately after the photoaging induction and the beginning of UV-B and treatment intervention overlapping period (UV-B co-stimulation period, Weeks 0–4), (2) Week 4, the end of the UV-B co-stimulation period (UV-B off period, Weeks 4–8). The

former represents the photoprotection effect, whereas the latter represents the recovery acceleration effect of each treatment regimen.

## 2.9 | Statistical analysis

Statistical analyses were performed using GraphPad Prism 7.0. The data are expressed as the mean  $\pm$  standard deviation (SD). Student's *t*-test (unpaired test at each moment and paired test in each group) was applied for statistical evaluation of the data. Intergroup *t*-tests and intragroup paired *t*-tests were performed for Weeks 2, 4, 6, and 8 to confirm the significance of MI reduction. Each mean difference was considered significant when the *p* value was  $<0.05$ .

## 3 | RESULTS

### 3.1 | Quantification of aqueous reactive species produced via LICAP treatment

A RONS assay using DCFH oxidation was performed to estimate the quantity of aqueous reactive species produced by LICAP treatment (Figure 3A,B). Initially, the level of RONS production increased proportionally with the treatment duration, showing a highly linear pattern (0–60 s). After that, the RONS level seemed to be saturated with a sluggish slope (60–120 s) (Figure 3A). The RONS quantification data of the initial phase (0–60 s) were closely fitted to a linear regression line ( $R^2=0.9737$ ) (Figure 3B).

### 3.2 | Cell viability test

The data of the WST-1 test were assessed using a colorimetric assay (Figure 4A–C). There was no significant change in viability during the

entire observation period, even when the treatment duration was extended to 5 min ( $p>0.05$ ).

### 3.3 | Visual inspection

After photoaging induction, the untreated group and the three treatment groups showed distinct hyperpigmentation on their dorsal skin compared to the healthy controls (Figure 5A,B). In the untreated group, UV-B-induced hyperpigmentation was sustained until the end of the study. There was no serious damage to the skin surface, except for some wrinkles, rhytides, and xerotic scales.

During the UV-B co-stimulation period, each change in skin pigmentation varied among the subjects; some subjects became lighter whereas the others did not change or became darker. However, most of the subjects in the three treatment groups recovered their skin color after the entire treatment period (UV-B co-stimulation period+UV-B off period). The overall pigment reduction effect seemed to be the most obvious in the LICAP+AA group, followed by that in the AA and LICAP groups.

### 3.4 | Melanin index

The melanin index was calculated based on the measurement data from the spectrophotometer (Figure 6A,B).

The mean MI value of each group was arrayed by weeks for intergroup comparison with the untreated control group (Figure 6A). At Weeks 4, 6, and 8, the mean MI values in the AA and LICAP+AA groups were significantly different from those in the untreated group. The detailed *p* values are listed in Table 1.

Each mean MI value was also arrayed by groups for intragroup comparisons (Figure 6B). In the untreated group, there was no significant change in the mean MI value after the overall treatment period (Weeks 0–8,  $p=0.198$ ) or after the UV-B off period (Weeks 4–8,

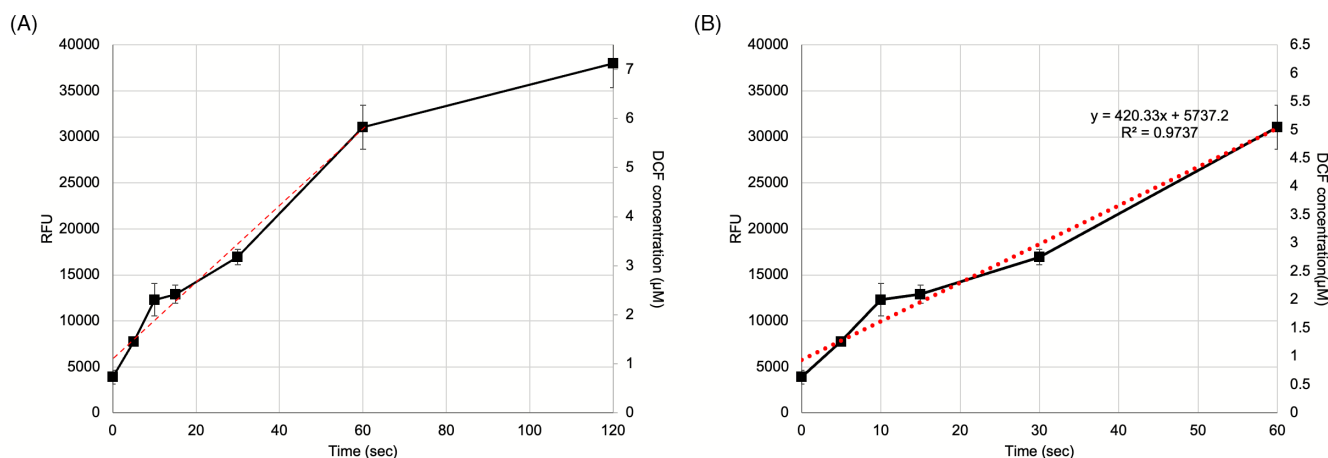


**FIGURE 3** Quantification data for aqueous reactive species production. (A) Time-scaled RONS production curves using the device. (B) Initial linearly increasing phase of the RONS production curve. Statistical significance was measured by comparison between the previous and present time points. (\* $p<0.05$ ; \*\* $p<0.01$ . DCF, 2', 7'-dichlorodihydrofluorescein; RFU, relative fluorescence units).

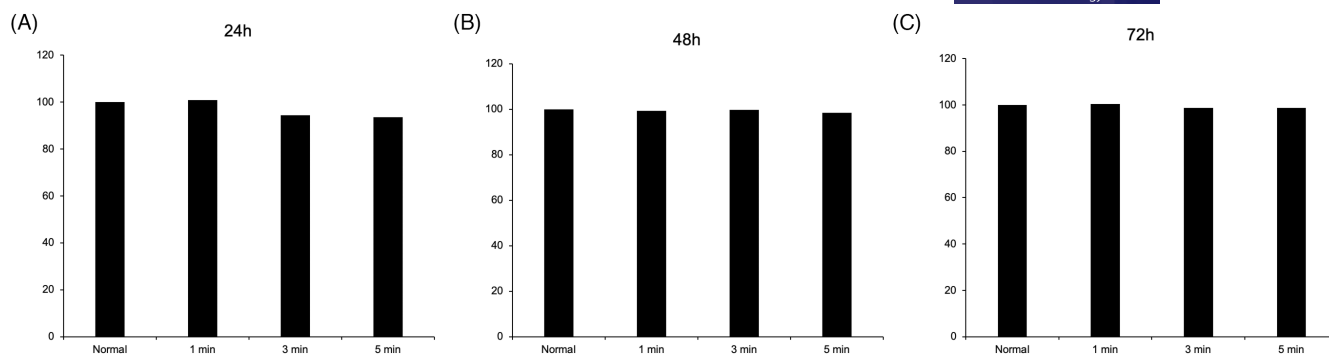


**FIGURE 4** Results of cell viability tests. Cell viability was measured at (A) 24h, (B) 48h, and (C) 72h after LICAP treatment. There was no significant change in cell viability within any of the subject groups during the entire observation period.

$p=0.179$ ). Notably, the mean MI value was significantly increased after the UV-B co-stimulation period (Weeks 0–4), reflecting the photodamage effect ( $p=0.0189$ ); in contrast, there was no significant change in the treatment groups (LICAP, AA, and LICAP+AA;  $p=0.684$ ,  $0.173$ , and  $0.356$ , respectively), indicating a photoprotective effect.

In the LICAP group, the mean MI value was significantly decreased after the overall treatment period (Weeks 0–8,  $p=0.0133$ ) and UV-B off period (Weeks 4–8,  $p=6.00 \times 10^{-3}$ ). The AA and LICAP+AA groups also showed significant decreases after the same periods as in the LICAP group, and there were some additional significant differences between various assessment time points (i.e., Weeks 0–6 in the AA group, Weeks 0–6, and Weeks 4–6 in the LICAP+AA group). The detailed  $p$  values are listed in Table 1.

The DPML was calculated (Table 2) and presented as line graphs to visualize the treatment efficacy more clearly (Figure 7A,B). The data of the intragroup paired  $t$ -test is noted on each graph because the calculation was based on the comparison between specific baseline and moment of interest in the same group.

The value of  $DPML_{0,8}$ , calculated from the comparison between Weeks 0 and 8 to reflect the overall pigment reduction effect during the whole treatment period, was the most remarkable in the LICAP+AA group ( $42.2\%$ ,  $p=8.83 \times 10^{-4}$ ), followed by that in the AA group ( $38.3\%$ ,  $p=0.0254$ ) and LICAP group ( $21.3\%$ ,  $p=0.0133$ ) (Figure 7A). It is likely that each value of  $DPML_{4,8}$ , calculated from the comparison between Weeks 4 and 8, to represent the pure treatment effect during the UV-B off period, was still significant in the same order as the  $DPML_{0,8}$  data (Figure 7B). The treatment was the most effective in the LICAP+AA group ( $36.3\%$ ,  $p=2.38 \times 10^{-4}$ ), followed by that in the AA group ( $30.2\%$ ,  $p=0.0254$ ) and LICAP group ( $26.6\%$ ,  $p=0.0254$ ).

## 4 | DISCUSSION

When first introduced in the medical field, the applications of CAP devices were focused on selectively eliminating RONS-vulnerable cells such as microorganisms and precancerous or cancer cells.<sup>24–29</sup>

These applications are based on the fact that CAP treatment can increase intracellular RONS levels and thus kill RONS-vulnerable cells. On the contrary, based on the growing body of evidence that low-dose CAP can induce cytoprotective mechanisms by activating pathways related to redox-sensitive transcription factors,<sup>8,9,11</sup> recent studies have focused on revealing the novel applications of CAP in a non-destructive manner, such as the treatment of chronic wounds, hair loss, eczema, pruritus, and wrinkles.<sup>4–7,10,30</sup>

The CAP treatment described in the present study is focused on generating a plasma density in a low range, which does not induce cytotoxic effects but still produces small amounts of intracellular RONS. Accordingly, I propose a new term *LICAP*, low-intensity cold atmospheric plasma, which refers to a physical plasma device designed to tune its plasma intensity in the low range and, thus, to mildly elevate the intracellular reactive species, the dose of which is below the cytotoxic level.

The results showed that the present LICAP treatment linearly increased the aqueous RONS level in the target solution until 60s (Figure 3A,B). RONS production increased with high linearity until it reached the saturation point. Thus, the present LICAP treatment seems to be able to tune the target RONS production level in a low, pre-saturated range by adjusting the treatment duration to 60s. Moreover, the cell viability data showed that LICAP did not induce cell death even when the treatment duration far exceeded the RONS saturation point of 60s (Figure 4A–C).

Topical AA application also showed photoprotective and skin-lightening effects on photodamaged skin (Figures 5–7) (Tables 1 and 2). The MI value in the AA group did not change significantly during the UV-B co-stimulation period ( $p=0.173$ ) and was significantly decreased during the UV-B off period ( $DPML_{4,8}$   $30.2\%$ ,  $p=0.0254$ ). The overall treatment efficacy,  $DPML_{0,8}$ , was  $38.3\%$  ( $p=4.99 \times 10^{-5}$ ). These results are understandable because AA, a well-known topical skin-lightening agent, prevents and restores UV-induced skin pigmentation by scavenging intracellular RONS.<sup>31,32</sup>

Interestingly, LICAP, a RONS producer, also showed photoprotective and skin-lightening effects similar to AA, and the MI value in the LICAP group did not change significantly during the UV-B co-stimulation period ( $p=0.684$ ) and was significantly decreased during the UV-B off period ( $DPML_{4,8}$   $26.6\%$ ,  $p=6.00 \times 10^{-3}$ ). The



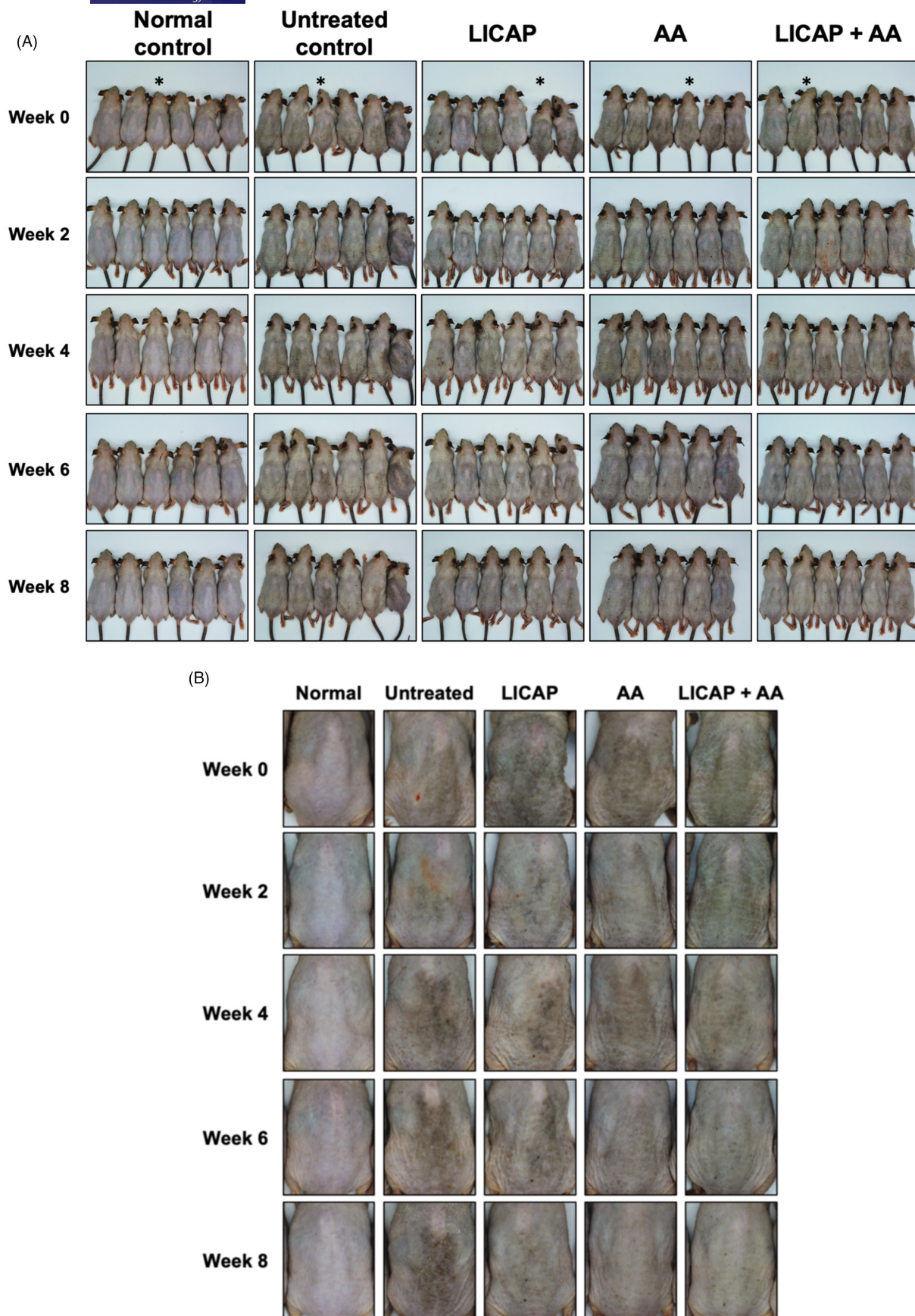


**FIGURE 5** Digital photographs for visual inspection. (A) Photographs of the study subjects. Representative images are marked (\*). (B) Photographs of representative subjects.

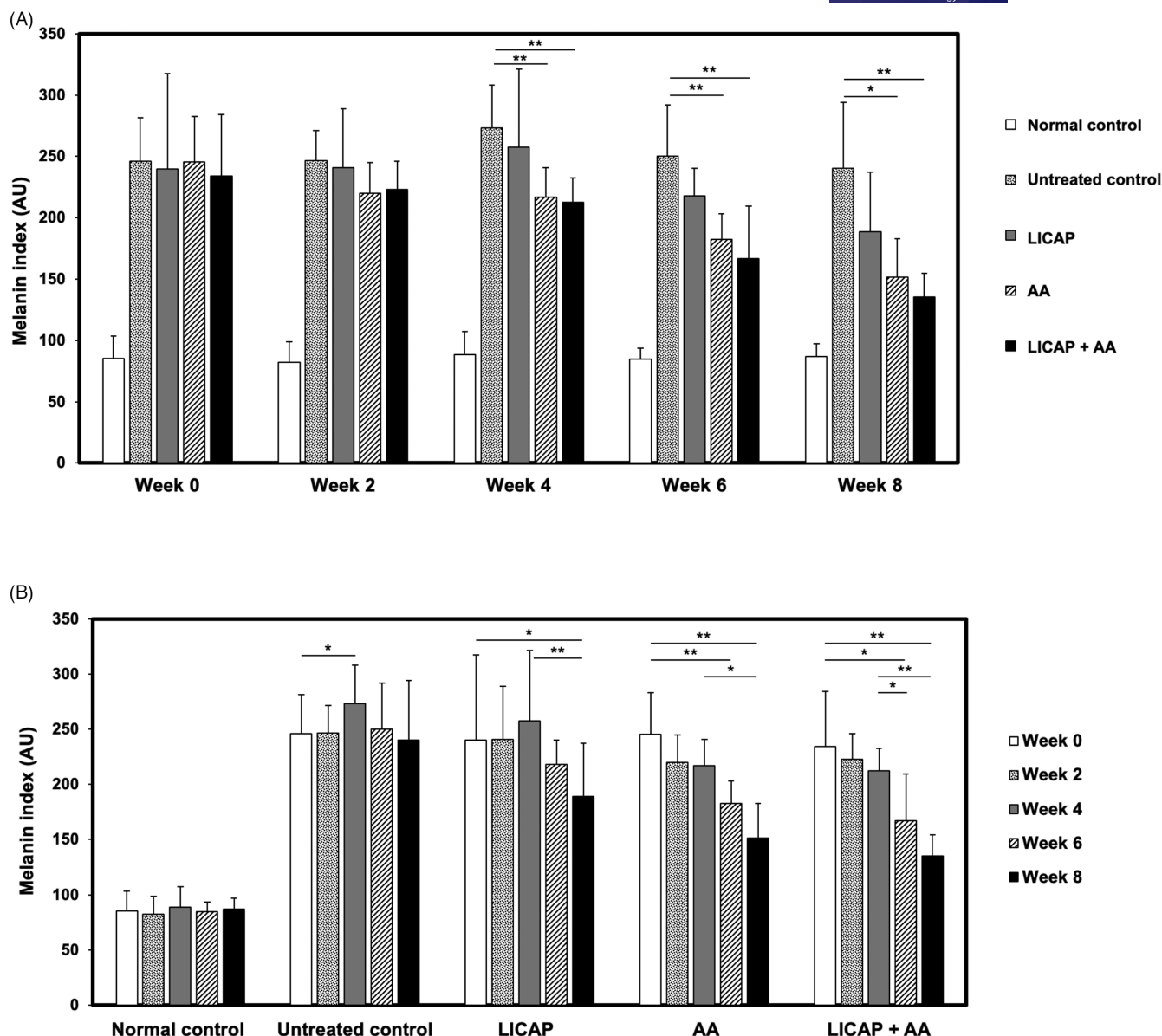


**FIGURE 6** Melanin index for quantitative analysis. The mean MI value of each group was arrayed by (A) weeks for intergroup comparison with the untreated control group and by (B) groups for intragroup comparison between the specific moments of interest and the baseline moments in the same group (\* $p < 0.05$ ; \*\* $p < 0.01$ ).

overall treatment efficacy,  $\text{DPMI}_{0.8}$ , was 21.3%. Although this was lower than that of the topical AA treatment, it was still significant ( $p = 0.0133$ ).

This might be one of the possible mechanisms by which LICAP treatment enhances the epidermal turnover rate. It has been previously reported that CAP treatment can enhance the proliferation of basal keratinocytes.<sup>33,34</sup> When the proliferation of basal keratinocytes is accelerated, newly proliferated keratinocytes replace the old ones that contain melanosomes, which is the key mechanism of various skin-lightening modalities including keratolytic agents, free fatty acids, and retinoic acid.<sup>35–37</sup>

Besides the effect explained above, it is quite possible that LICAP treatment might paradoxically lower the oxidative burden in cells; that is, it might induce hormesis in skin cells.<sup>8,38</sup> The term

*hormesis* refers to a biphasic dose response characterized by a low-dose beneficial effect and a high-dose toxic effect.<sup>39,40</sup> Low-dose CAP irradiation can activate the pathway related to Nrf2, a key redox-sensitive transcription factor, to upregulate endogenous antioxidants.<sup>11,41</sup> Interestingly, Hwang et al. recently revealed that the effect of increased antioxidant buffering capacity by low-dose CAP treatment was sufficient to lower the intracellular RONS level in UV-irradiated skin cells.<sup>10</sup>

Lastly, keratinocytes might undergo a selective autophagy process, via which the accumulated melanosomes are cleared in case the Nrf2-related pathway is activated by the present LICAP treatment.<sup>15,16</sup> The key adaptor protein for selective autophagy, p62, has been reported as one of the molecules upregulated by Nrf2 activation.<sup>12</sup> Moreover, p62 forms a positive feedback loop with its

TABLE 1 Melanin index (arbitrary units).

		Week 0	Week 2	Week 4	Week 6	Week 8
Normal control	<i>n</i>	6	6	6	6	6
	Mean±SD	85.5±18.1	82.1±16.8	88.6±18.7	84.9±8.51	86.9±10.1
	<i>p</i> Value					
	vs. Week 0	–	0.358	0.564	0.950	0.866
	vs. Week 4	–	–	–	0.709	0.846
Untreated control	<i>n</i>	6	6	6	6	6
	Mean±SD	246±35.5	241±24.9	285±34.8	250±41.8	215±53.8
	<i>p</i> Value					
	vs. Week 0	–	0.595	0.0189*	0.800	0.198
	vs. Week 4	–	–	–	0.0693	0.179
LICAP	<i>N</i>	6	6	6	5 <sup>a</sup>	5 <sup>a</sup>
	Mean±SD	252±77.6	241±48.3	257±64.1	218±22.3	189±48.2
	<i>p</i> Value					
	vs. Week 0	–	0.360	0.684	0.215	0.0133*
	vs. Week 4	–	–	–	0.0774	6.00×10 <sup>-3**</sup>
AA	<i>N</i>	6	6	6	6	6
	Mean±SD	248±37.4	220±24.9	217±24.3	183±20.7	159±31.7
	<i>p</i> Value					
	vs. Week 0	–	0.222	0.173	8.00×10 <sup>-3**</sup>	4.99×10 <sup>-5**</sup>
	vs. Week 4	–	–	–	0.0512	0.0254*
LICAP+AA	<i>n</i>	6	6	6	6	6
	Mean±SD	234±49.9	223±23.1	212±20.1	167±42.6	135±19.1
	<i>p</i> Value					
	vs. Week 0	–	0.582	0.356	0.0186*	8.83×10 <sup>-4**</sup>
	vs. Week 4	–	–	–	0.0327*	2.38×10 <sup>-4**</sup>
AA	<i>N</i>	6	6	6	6	6
	Mean±SD	248±37.4	220±24.9	217±24.3	183±20.7	159±31.7
	<i>p</i> Value					
	vs. Week 0	–	0.222	0.173	8.00×10 <sup>-3**</sup>	4.99×10 <sup>-5**</sup>
	vs. Week 4	–	–	–	0.0512	0.0254*
LICAP+AA	<i>n</i>	6	6	6	6	6
	Mean±SD	234±49.9	223±23.1	212±20.1	167±42.6	135±19.1
	<i>p</i> Value					
	vs. Week 0	–	0.582	0.356	0.0186*	8.83×10 <sup>-4**</sup>
	vs. Week 4	–	–	–	0.0327*	2.38×10 <sup>-4**</sup>
AA	<i>N</i>	6	6	6	6	6
	Mean±SD	248±37.4	220±24.9	217±24.3	183±20.7	159±31.7
	<i>p</i> Value					
	vs. Week 0	–	0.222	0.173	8.00×10 <sup>-3**</sup>	4.99×10 <sup>-5**</sup>
	vs. Week 4	–	–	–	0.0512	0.0254*
LICAP+AA	<i>n</i>	6	6	6	6	6
	Mean±SD	234±49.9	223±23.1	212±20.1	167±42.6	135±19.1
	<i>p</i> Value					
	vs. Week 0	–	0.582	0.356	0.0186*	8.83×10 <sup>-4**</sup>
	vs. Week 4	–	–	–	0.0327*	2.38×10 <sup>-4**</sup>

<sup>a</sup>One subject in group C died in Week 5 because of an unspecified cause, which seemed not to be related to the treatment. The missing data were replaced by the rule of the last observation carried forward (LOCF) method.

\**p*<0.05; \*\**p*<0.001.

	DPMI <sub>0,4</sub>	DPMI <sub>0,8</sub>	DPMI <sub>4,8</sub>
Untreated control	-11.1% ( <i>p</i> =0.0189)*	2.46% ( <i>p</i> =0.198)	12.2% ( <i>p</i> =0.179)
LICAP	-7.26% ( <i>p</i> =0.684)	21.3% ( <i>p</i> =0.0133*)	26.6% ( <i>p</i> =6.00×10 <sup>-3**</sup> )
AA	9.25% ( <i>p</i> =0.173)	38.3% ( <i>p</i> =4.99×10 <sup>-5**</sup> )	30.2% ( <i>p</i> =0.0254*)
LICAP+AA	11.7% ( <i>p</i> =0.356)	42.2% ( <i>p</i> =8.83×10 <sup>-4**</sup> )	36.3% ( <i>p</i> =2.38×10 <sup>-4**</sup> )

\**p*<0.05; \*\**p*<0.001.

TABLE 2 Decreased percentage of melanin index (DPMI).

	DPMI <sub>0,4</sub>	DPMI <sub>0,8</sub>	DPMI <sub>4,8</sub>
Untreated control	-11.1% ( <i>p</i> =0.0189)*	2.46% ( <i>p</i> =0.198)	12.2% ( <i>p</i> =0.179)
LICAP	-7.26% ( <i>p</i> =0.684)	21.3% ( <i>p</i> =0.0133*)	26.6% ( <i>p</i> =6.00×10 <sup>-3**</sup> )
AA	9.25% ( <i>p</i> =0.173)	38.3% ( <i>p</i> =4.99×10 <sup>-5**</sup> )	30.2% ( <i>p</i> =0.0254*)
LICAP+AA	11.7% ( <i>p</i> =0.356)	42.2% ( <i>p</i> =8.83×10 <sup>-4**</sup> )	36.3% ( <i>p</i> =2.38×10 <sup>-4**</sup> )

\**p*<0.05; \*\**p*<0.001.

transcription factor Nrf2, as it competitively inhibits Keap1, which sequesters Nrf2 in the cytoplasm.<sup>13,14</sup>

The treatment effect of the concurrent therapy was found to be superior to that of both single therapies. MI was decreased by 42.2% in the LICAP+AA group during the whole treatment period, whereas LICAP and AA reduced MI by 26.6% and 30.2%, respectively. This

suggests that both therapies do not interfere with each other at any rate and may have additive or synergistic effects through the mechanisms explained below (Figure 8).

It is more likely that LICAP treatment enhanced the diffusion of AA into the deeper skin. Recently, several studies have suggested that CAP can enhance drug diffusion into deeper tissues



**FIGURE 7** Percent decrease in melanin index by time. Each percentage was calculated as the proportion of the melanin index decrease based on the melanin index at (A) Week 0 or (B) Week 4.

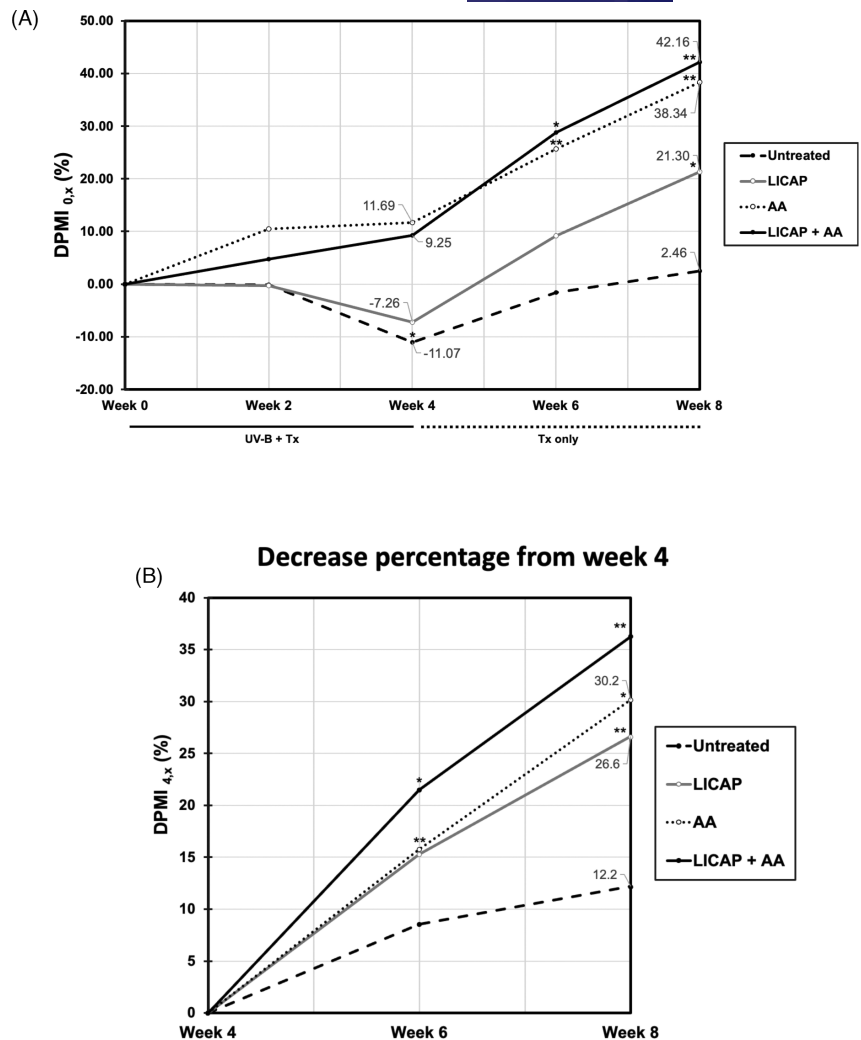
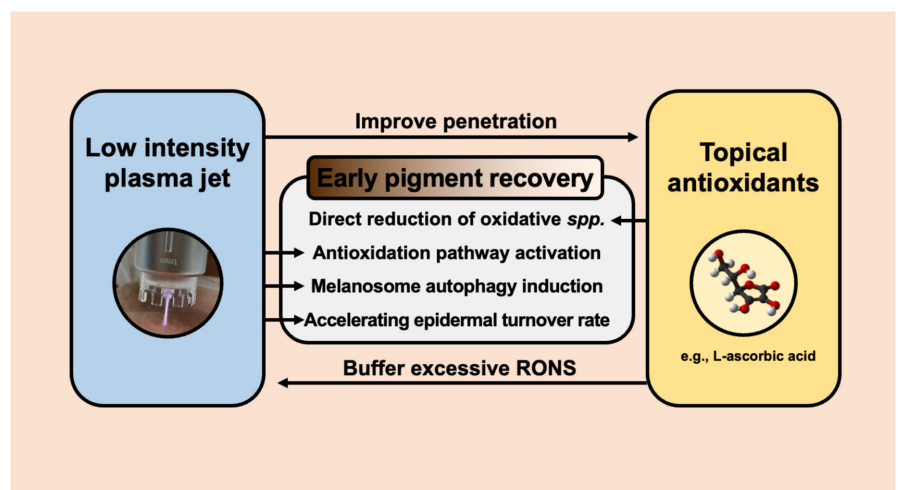


**FIGURE 8** Schematic explaining the mutually complementary effect of LICAP treatment and topical AA application on pigmentation recovery after photodamage.



via both intra- and intercellular routes.<sup>42</sup> CAP downregulates the expression of cell adhesion molecules,<sup>43–46</sup> induces detachment of individual cells,<sup>47,48</sup> and increases cell membrane permeability.<sup>49,50</sup> Therefore, the antecedent LICAP treatment might have facilitated the topical AA treatment to overcome the critical limitation of skin penetration.

Additionally, the subsequent topical AA application might have offset the remnant RONS produced from the antecedent LICAP treatment. Although the present LICAP treatment was proven to have no effect on cell viability, the use of a potent antioxidant agent may still reduce the possibility of overloaded oxidative stress in cells. Therefore, it is possible that the pigment reduction effects of

LICAP treatment and topical antioxidant AA application are mutually complementary.

To the best of our knowledge, the present study is the first prospective animal study to observe the effect of LICAP treatment on pigment reduction in photoaged skin in a hairless mouse model. However, there are some limitations in that it was a relatively small-sized animal study and there was only one parameter setting for LICAP treatment in the in vivo study. Although the data indicate that the plasma density was low enough to avoid cell death, the present data are not sufficient to reveal the exact therapeutic range for clinical use in terms of efficacy and safety. Further investigations are, thus, needed to set the ideal treatment protocol based on carefully accumulated clinical experiences.

In summary, the LICAP treatment used in the present study can tune RONS production in the target solution in a low, pre-saturated range and does not result in cell death even with prolonged treatment duration. The LICAP treatment showed a photoprotective effect against UV irradiation and accelerated the restoration of skin color after photoaging in a hairless mouse model, similar to topical AA treatment. The combination of both therapies was more effective than the single therapies. However, further investigations are needed for the clinical use of this protocol.

#### AUTHOR CONTRIBUTIONS

Ga Ram Ahn: Conceptualization, investigation, original draft. Hyung Joon Park: Conceptualization, methodology, investigation, original draft. Young Gue Koh: Review and editing manuscript, investigation. Ka Ram Kim: Review and editing manuscript, investigation. Yu Jin Kim: Conceptualization, methodology, investigation. Jung Ok Lee: Conceptualization, methodology, investigation, review and editing manuscript. Joon Seok: In vivo experiment design, data analysis, supervision. Kwang Ho Yoo: Review and editing manuscript, investigation, supervision. Kyu Back Lee, Beom Joon Kim: Conceptualization, manuscript review, supervision.

#### ACKNOWLEDGEMENTS

This work was supported by the Institute of Information & Communications Technology Planning & Evaluation (IITP) grant funded by the Korean government (MSIT) (No. 2021-0-01074, Development of Intelligent Plasma Medical Device Applying User Data Platform Technology Project).

#### CONFLICT OF INTEREST STATEMENT

One of the authors, Ga Ram Ahn, declares a non-financial interest due to his first-degree relative works for the cooperation that provided the test device. All other authors declare no conflicts of interest.

#### DATA AVAILABILITY STATEMENT

The data that support the findings of this study are available from the corresponding author upon reasonable request.

#### ORCID

Ga Ram Ahn  <https://orcid.org/0000-0002-5696-4699>

Young Gue Koh  <https://orcid.org/0000-0002-6376-0328>

#### REFERENCES

1. D'Alba L, Shawkey MD. Melanosomes: biogenesis, properties, and evolution of an ancient organelle. *Physiol Rev*. 2019;99(1):1-19. doi:10.1152/physrev.00059.2017
2. Metelmann HR, von Woedtke T, Weltmann KD. In: Metelmann HR, von Woedtke T, Weltmann KD, eds. *Comprehensive Clinical Plasma Medicine: Cold Physical Plasma for Medical Application*. Springer International Publishing; 2018. doi:10.1007/978-3-319-67627-2
3. Gentile RD. Cool atmospheric plasma (j-plasma) and new options for facial contouring and skin rejuvenation of the heavy face and neck. *Facial Plast Surg*. 2018;34(1):66-74. doi:10.1055/s-0037-1621713
4. Bernhardt T, Semmler ML, Schäfer M, Bekeschus S, Emmert S, Boeckmann L. Plasma medicine: applications of cold atmospheric pressure plasma in dermatology. *Oxid Med Cell Longev*. 2019;2019:3873928. doi:10.1155/2019/3873928
5. Gan L, Jiang J, Duan JW, et al. Cold atmospheric plasma applications in dermatology: A systematic review. *J Biophotonics*. 2021;14(3):e202000415. doi:10.1002/jbio.202000415
6. Friedman PC. Cold atmospheric pressure (physical) plasma in dermatology: where are we today? *Int J Dermatol*. 2020;59(10):1171-1184. doi:10.1111/ijd.15110
7. Busco G, Robert E, Chettouh-Hammas N, Pouvesle JM, Grillon C. The emerging potential of cold atmospheric plasma in skin biology. *Free Radic Biol Med*. 2020;161:290-304. doi:10.1016/j.freeradbiomed.2020.10.004
8. Szili EJ, Harding FJ, Hong SH, Herrmann F, Voelcker NH, Short RD. The hormesis effect of plasma-elevated intracellular ROS on HaCaT cells. *J Phys D Appl Phys*. 2015;48(49):495401. doi:10.1088/0022-3727/48/49/495401
9. Privat-Maldonado A, Schmidt A, Lin A, et al. ROS from physical plasmas: redox chemistry for biomedical therapy. *Oxid Med Cell Longev*. 2019;2019:1-29. doi:10.1155/2019/9062098
10. Hwang SG, Kim JH, Jo SY, Kim YJ, Won CH. Cold atmospheric plasma prevents wrinkle formation via an antiaging process. *Plasma Med*. 2020;10(2):91-102. doi:10.1615/PlasmaMed.2020034810
11. Schmidt A, Bekeschus S. Redox for repair: cold physical plasmas and nrf2 signaling promoting wound healing. *Antioxidants*. 2018;7(10):1-17. doi:10.3390/antiox7100146
12. Liu WJ, Ye L, Huang WF, et al. p62 links the autophagy pathway and the ubiquitin-proteasome system upon ubiquitinated protein degradation. *Cell Mol Biol Lett*. 2016;21(1):29. doi:10.1186/s11658-016-0031-z
13. Jain A, Lamark T, Sjøttem E, et al. p62/SQSTM1 is a target gene for transcription factor NRF2 and creates a positive feedback loop by inducing antioxidant response element-driven gene transcription. *J Biol Chem*. 2010;285(29):22576-22591. doi:10.1074/jbc.M110.118976
14. Komatsu M, Kurokawa H, Waguri S, et al. The selective autophagy substrate p62 activates the stress responsive transcription factor Nrf2 through inactivation of Keap1. *Nat Cell Biol*. 2010;12(3):213-223. doi:10.1038/ncb2021
15. Murase D, Hachiya A, Takano K, et al. Autophagy has a significant role in determining skin color by regulating melanosome degradation in keratinocytes. *J Invest Dermatol*. 2013;133(10):2416-2424. doi:10.1038/ijd.2013.165
16. Kim JY, Kim J, Ahn Y, et al. Autophagy induction can regulate skin pigmentation by causing melanosome degradation in keratinocytes and melanocytes. *Pigment Cell Melanoma Res*. 2020;33(3):403-415. doi:10.1111/pcmr.12838
17. Campo-Sabariz J, Garcia-Vara A, Moral-Anter D, et al. Hydroxy-Selenomethionine, an organic selenium source, increases selenoprotein expression and positively modulates the inflammatory response of lps-stimulated macrophages. *Antioxidants*. 2022;11(10). doi:10.3390/antiox11101876
18. Kumawat M, Madhyastha H, Singh M, Revaprasadu N, Srinivas SP, Daima HK. Double functionalized haemocompatible silver

- nanoparticles control cell inflammatory homeostasis. *PLoS One*. 2022;17:1-19. doi:10.1371/journal.pone.0276296
19. Huh CH, Ki S, Park JY, Lim JG, Eun HC, Park KC. A randomized, double-blind, placebo-controlled trial of vitamin C iontophoresis in melasma. *Dermatology*. 2003;206(4):316-320. doi:10.1159/000069943
  20. Ebihara M, Akiyama M, Ohnishi Y, Tajima S, Komata KI, Mitsui Y. Iontophoresis promotes percutaneous absorption of L-ascorbic acid in rat skin. *J Dermatol Sci*. 2003;32(3):217-222. doi:10.1016/S0923-1811(03)00105-1
  21. Sobhi RM, Sobhi AM. A single-blinded comparative study between the use of glycolic acid 70% peel and the use of topical nanosome vitamin C iontophoresis in the treatment of melasma. *J Cosmet Dermatol*. 2012;11(1):65-71. doi:10.1111/j.1473-2165.2011.00599.x
  22. Jung EC, Zhu H, Zou Y, et al. Effect of ultrasound and heat on percutaneous absorption of L-ascorbic acid: human in vitro studies on Franz cell and Petri dish systems. *Int J Cosmet Sci*. 2016;38(6):646-650. doi:10.1111/ics.12350
  23. Zasada M, Markiewicz A, Drożdż Z, Mosińska P, Erkiert-Polguj A, Budzisz E. Preliminary randomized controlled trial of antiaging effects of L-ascorbic acid applied in combination with no-needle and microneedle mesotherapy. *J Cosmet Dermatol*. 2019;18(3):843-849. doi:10.1111/jocd.12727
  24. Filipić A, Gutierrez-Aguirre I, Primc G, Mozetič M, Dobnik D. Cold plasma, a new hope in the field of virus inactivation. *Trends Biotechnol*. 2020;38(11):1278-1291. doi:10.1016/j.tibtech.2020.04.003
  25. Chen Y, Chen Y, Chung W, Tong B, Chang MB. Evaluation of the effectiveness of nonthermal plasma disinfection. *Environ Technol*. 2020;41(21):2795-2805. doi:10.1080/09593330.2019.1583289
  26. Reitberger HH, Czugała M, Chow C, et al. Argon cold plasma—a novel tool to treat therapy-resistant corneal infections. *Am J Ophthalmol*. 2018;190:150-163. doi:10.1016/j.ajo.2018.03.025
  27. Nguyen L, Lu P, Boehm D, et al. Cold atmospheric plasma is a viable solution for treating orthopedic infection: a review. *Biol Chem*. 2018;400(1):77-86. doi:10.1515/hsz-2018-0235
  28. Yan D, Sherman JH, Keidar M. Cold atmospheric plasma, a novel promising anti-cancer treatment modality. *Oncotarget*. 2017;8(9):15977-15995. doi:10.18632/oncotarget.13304
  29. Dai X, Bazaka K, Thompson EW, Ostrikov KK. Cold atmospheric plasma: a promising controller of cancer cell states. *Cancers (Basel)*. 2020;12(11). doi:10.3390/cancers12113360
  30. Heinlin J, Isbary G, Stolz W, et al. A randomized two-sided placebo-controlled study on the efficacy and safety of atmospheric non-thermal argon plasma for pruritus. *J Eur Acad Dermatol Venereol*. 2013;27(3):324-331. doi:10.1111/j.1468-3083.2011.04395.x
  31. Sanadi RM, Deshmukh RS. The effect of Vitamin C on melanin pigmentation – A systematic review. *J Oral Maxillofac Pathol*. 2017;24(2):374-382. doi:10.4103/jomfp.JOMFP\_207\_20
  32. Panich U, Tangsupa-a-nan V, Onkoksoong T, et al. Inhibition of UVA-mediated melanogenesis by ascorbic acid through modulation of antioxidant defense and nitric oxide system. *Arch Pharm Res*. 2011;34(5):811-820. doi:10.1007/s12272-011-0515-3
  33. García JL, Asadinezhad A, Pachernik J, et al. Cell proliferation of HaCaT keratinocytes on collagen films modified by argon plasma treatment. *Molecules*. 2010;15(4):2845-2856. doi:10.3390/molecules15042845
  34. Hasse S, Duong Tran T, Hahn O, et al. Induction of proliferation of basal epidermal keratinocytes by cold atmospheric-pressure plasma. *Clin Exp Dermatol*. 2016;41(2):202-209. doi:10.1111/ced.12735
  35. Shenoy A, Madan R. Post-Inflammatory Hyperpigmentation: A Review of Treatment Strategies. *J Drugs Dermatol*. 2020;19(8):763-768. doi:10.36849/JDD.2020.4887
  36. Couteau C, Coiffard L. Overview of skin whitening agents: drugs and cosmetic products. *Cosmetics*. 2016;3(3):27. doi:10.3390/cosmetics3030027
  37. Burger P, Landreau A, Azoulay S, Michel T, Fernandez X. Skin whitening cosmetics: feedback and challenges in the development of natural skin lighteners. *Cosmetics*. 2016;3(4):36. doi:10.3390/cosmetics3040036
  38. Privat-Maldonado A, Schmidt A, Lin A, et al. ROS from physical plasmas: redox chemistry for biomedical therapy. *Oxid Med Cell Longev*. 2019;2019. doi:10.1155/2019/9062098
  39. Sthijns MMJPE, Weseler AR, Bast A, Haenen GRMM. Time in redox adaptation processes: From evolution to hormesis. *Int J Mol Sci*. 2016;17(10):1649. doi:10.3390/ijms17101649
  40. Oliveira MF, Geijs MA, França TFA, Moreira DC, Hermes-Lima M. Is “preparation for oxidative stress” a case of physiological conditioning hormesis? *Front Physiol*. 2018;9:1-6. doi:10.3389/fphys.2018.00945
  41. Schmidt A, von Woedtke T, Vollmar B, Hasse S, Bekeschus S. Nrf2 signaling and inflammation are key events in physical plasma-spurred wound healing. *Theranostics*. 2019;9(4):1066-1084. doi:10.7150/thno.29754
  42. Wen X, Xin Y, Hamblin MR, Jiang X. Applications of cold atmospheric plasma for transdermal drug delivery: a review. *Drug Deliv Transl Res*. 2020;37. doi:10.1007/s13346-020-00808-2
  43. Haertel B, Wende K, von Woedtke T, Weltmann KD, Lindequist U. Non-thermal atmospheric-pressure plasma can influence cell adhesion molecules on HaCaT-keratinocytes. *Exp Dermatol*. 2011;20(3):282-284. doi:10.1111/j.1600-0625.2010.01159.x
  44. Haertel B, Hahnel M, Blackert S, Wende K, von Woedtke T, Lindequist U. Surface molecules on HaCaT keratinocytes after interaction with non-thermal atmospheric pressure plasma. *Cell Biol Int*. 2012;36(12):1217-1222. doi:10.1042/CBI20120139
  45. Haertel B, Strassenburg S, Oehmigen K, Wende K, von Woedtke T, Lindequist U. Differential influence of components resulting from atmospheric-pressure plasma on integrin expression of human HaCaT keratinocytes. *Biomed Res Int*. 2013;2013:761451. doi:10.1155/2013/761451
  46. Choi JH, Nam SH, Song YS, et al. Treatment with low-temperature atmospheric pressure plasma enhances cutaneous delivery of epidermal growth factor by regulating E-cadherin-mediated cell junctions. *Arch Dermatol Res*. 2014;306(7):635-643. doi:10.1007/s00403-014-1463-9
  47. Hoentsch M, von Woedtke T, Weltmann KD, Nebe JB. Time-dependent effects of low-temperature atmospheric-pressure argon plasma on epithelial cell attachment, viability and tight junction formation in vitro. *J Phys D Appl Phys*. 2011;45(2):25206.
  48. Hoentsch M, Bussiahn R, Rebl H, et al. Persistent effectivity of gas plasma-treated, long time-stored liquid on epithelial cell adhesion capacity and membrane morphology. *PLoS One*. 2014;9(8):e104559. doi:10.1371/journal.pone.0104559
  49. Haralambiev L, Nitsch A, Eienkel R, et al. The effect of cold atmospheric plasma on the membrane permeability of human osteosarcoma cells. *Anticancer Res*. 2020;40(2):841-846. doi:10.21873/anticancer.14016
  50. Yusupov M, van der Paal J, Neyts EC, Bogaerts A. Synergistic effect of electric field and lipid oxidation on the permeability of cell membranes. *Biochim Biophys Acta Gen Subj*. 2017;1861(4):839-847. doi:10.1016/j.bbagen.2017.01.030

**How to cite this article:** Ahn GR, Park HJ, Koh YG, et al. The effect of low-intensity cold atmospheric plasma jet on photoaging-induced hyperpigmentation in mouse model. *J Cosmet Dermatol*. 2023;00:1-11. doi:10.1111/jocd.15778